# SPECTRUM-BASED FRACTAL ANALYSIS OF MYOELECTRIC SIGNALS USING PIECEWISE STATISTICALLY SELF-AFFINE POWER-LAWS

*Mehran Talebinejad[1,2], Adrian D.C. Chan[2], and Ali Miri[1]*
[1]School of Information Technology and Engineering, University of Ottawa, CANADA
[2]Department of Systems and Computer Engineering, Carleton University, CANADA

**Abstract** In this paper we present a novel set of statistically self-affine power laws and an algorithm for parameter estimation of a piecewise power law combination. The piecewise combination is applicable to irregular power spectral densities which do not follow the classic form of strict statistical self-affinity. The piecewise modeling also enables local analysis with variable magnification factors, which is very informative about the spectral distribution of the texture. Results of an experiment on simulated myoelectric signals are also presented. In this experiment, two conditions in which a single power law results in large errors are investigated. The results show that extension of the modeling to a piecewise combinational approach improves the accuracy and results in a better representation of the power spectrum. The results also show a great potential for applications of this approach to a wide variety of bio-signals with a multi-fractal behavior, which is very close to combinational mono-fractals in texture.

## 1. INTRODUCTION

Spectral dimensions, in form of the dimension of a random scaling fractal is potentially accurate for noise types whose power spectrum exhibits $1/f^{\alpha}$ behavior and strict self-affinity; that is, the magnitude of the power spectrum changes linearly with respect to the frequency in a bi-logarithmic plot. This implies that as we zoom into the signal, the distribution of the samples does not change; the samples are only subjected to some uniform scaling of the distribution at all frequencies. In such signals, a $1/f^{\alpha}$ power spectral estimation method, using a single line, provides a very good representation. This approach for extracting a spectral slope [1], however, is not directly applicable to most bio-signals, which exhibit non-linear spectral behavior, such as electroencephalography, myoelectric, and speech signals. In other words, textural information is not well represented using a single level complexity measure in form of the $1/f^{\alpha}$ approach. This has led to partitioning algorithms for modeling the power spectrum with piecewise linear models. Although dividing nonlinear surfaces to several lines might provide a good representation with low modeling errors, high dimensionality of the resulting spectral slopes make this approach computationally expensive. Moreover, these partitioning algorithms are not mathematically justified to be optimal for representing a fractal behavior, as they are optimized for power spectrum modeling. The resulting fractal indicators do not represent a unified fractal profile, as they are unrelated to one another. Linear partitioning results in arbitrary lines which do not mathematically represent a fractal, and may also be invalid for other partition frequency intervals.

We have previously introduced a novel power law [2, 3] which represents a general statistically self-affine power spectrum. A general behavior that can be represented by this power law is very close to characteristics of many bio-signals, such as electroencephalography or myoelectric signals, which originate from a strongly non-linear summation of smaller components (neural firings or motor unit action potentials). In [5] it is shown that parameters extracted according to this power law are sensitive to the effects of contractile force and joint angle; meanwhile, they are independent from the changes of the muscle fiber conduction velocity (CV), an indicator of muscular fatigue.

In this paper, we present a partitioning algorithm for piecewise general self-affine power laws. A single power law may not provide a sufficient representation of the spectrum when it is compressed or skewed (e.g. MES with low CV, or high depth motor units). The partitioning algorithm improves modeling accuracy by enabling the description of localized characteristics. This is similar to what motivated partition algorithms for the linear $1/f^{\alpha}$ approach; however, this algorithm assumes a fixed characteristic frequency for each partition, so the extracted indicators of each partition are computed as part of one profile. The actual profile is described with multiple indicators rather than several partitions represented with different exponents as with the linear $1/f^{\alpha}$ approach. This new partitioning algorithm is applied to simulated MESs, with results demonstrating improved modeling accuracy.

## 2. GENERAL SELF-AFFINITY AND THE PARTITIONING ALGORITHM

The power spectrum of a general self-affine signal could be represented in this form,

$$P_E(f) = c\left(\frac{f}{f_0}\right)^{2g} \Bigg/ \left(\left(\frac{f}{f_0}\right)^2 + 1\right)^{q+g} \qquad (1)$$

in Eq.(1), $c$ is a scaling factor related to the power of the signal, $q$ and $g$ are high and low frequency indicators, and $f_0$ is a characteristic frequency representing shifts among the distributions [1]. This power law is regulated by more than one exponent. Multiple exponents allow this power law to represent self-affine profiles in which zooming into the signal distribution of the samples is not changed but they are non-uniformly scaled and shifted in frequency in this form,

$$\Pr[s(t, f_0)] = \frac{\lambda^g}{\lambda^q} \Pr[s(\lambda t, f_0/\lambda)] \qquad (2)$$

in Eq.(2), $s$ is a 1-D temporal general self-affine signal and the probability distribution functions Pr[·] are simply scaled and shifted when the time is scaled by λ (zooming into $s$).

This power law can provide a fairly accurate representation for the power spectrum of MESs [2]. For example, the MES power spectrum, with characteristics of a moderate biceps contraction (CV = 5.5 m/s) and its modeled version using the general self-affine power law, differs by 2.0 % of the total signal power Fig. (1)).

The error rate represents a curve fitting error; however, since we are using Eq.(1) for curve fitting, the error rate is also a measure of self-affinity. This is why we are interested in Eq.(1) as a fundamental measure rather than using other curves, which might result in a lower error rate. Also, note that this performance (low error rates) is limited to frequency ranges which are not close to the low cut off frequency around the DC level. This frequency range used in Fig.(1) is 30-300 Hz. Accuracy of this model decreases dramatically if the frequency range 1-30 Hz is included (error rate increases to 11.7 %). This suggests that the spectral behavior near the cut off frequency is representing different textural characteristics, which are not similar to the rest of the frequencies. There are also cases in which the degree of self-affinity of the MES power spectrum is decreased with respect to one single power law, where the whole power spectrum is modeled as a mono-fractal. We do not intend to investigate the effects of the MES parameters on the degree of the self-affinity, in this work; rather, to motivate a novel partitioning algorithm and piecewise modeling, we are introducing the piecewise power law in the context of two conditions to demonstrate its effectiveness: 1) low muscle fiber CV [4, 5]; and 2) high depth of detected active motor units (MUs). In both cases, a single power law results in large modeling errors. In the first case, a low CV which might be caused by muscular fatigue and/or disorders of a muscle [3, 4], resulting in a significant shift of the MES power spectrum towards lower frequencies [4, 5]. This phenomenon also causes a compressed low frequency behavior in the power spectrum, which is not effectively nor accurately characterized by a single power law as shown in Fig.(1) when CV = 3 m/s. In the second case, a high depth of the detected active MUs, which could be caused by an acute joint angle [2, 3], results in a skew of the higher power spectrum that cannot be accurately modeled by a single power law. In both cases, the error is more than 10 % of the total power of the signal.

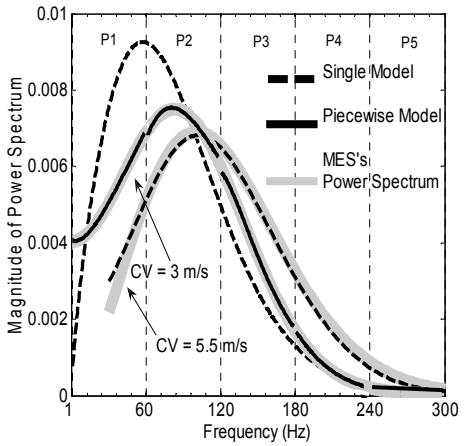


Figure 1: MES power spectrum with CVs of 5.5 and 3 m/s. A single power law model adequately models the CV = 5.5 m/s MES spectrum but is highly erroneous for CV = 3 m/s. The piecewise power law modeling, with partitions P1 to P5, is very accurate for the CV = 3 m/s MES spectrum.

To improve the modeling capabilities of the power law, we introduce a partitioning algorithm and model each partition of the spectrum by a single power law in the form of the Eq.(1). Each partition is assumed to have characteristic frequencies related to its local power distribution. The most important underlying factor in this algorithm is the fact that corresponding power laws of the all partitions add up to represent the whole power spectrum. This is in contrast to linear models which are only valid in their associated partition. In other words, the presented algorithm results in partition models that are only differ in their characteristic frequency and magnification. This novel algorithm allows the application of a single model that can be shifted and magnified towards different distributions for local analysis. Unlike linear piecewise model, the resulting model parameters are related and represent a unified fractal profile. The algorithm is formulated as follows.

**Step 1:** The power spectrum is modeled by a single power law which is scaled by the order of the partitioning (i.e. number of the partitions) in this form,

$$P_{pw}(f) = N \cdot P_E(f) \quad (3)$$

in Eq.(3), $N$ is the order of partitioning, $P_E(f)$ is a single power law as in Eq.(1) and $P_{pw}(f)$ is the piecewise combinational power law which is obtained in this step. The parameters of $P_{pw}(f)$ are estimated using the algorithm presented in [2]. In this algorithm an error is defined in this form,

$$e(q,g,c,f_0) = \sum_{i=1}^{M_T} \left(P(f_i) - P_{pw}(f_i)\right)^2 \quad (4)$$

in Eq.(4), $P(f)$ is the actual MES power spectrum, $P_{pw}(f)$ is the estimated version using the Eq.(3) and $M_T$ is the total number of samples in the power spectrum. It should be noted that the order of the partitioning $N$ is lumped into the scaling factor and is treated as an unknown; its value is determined in the next step.

**Step 2:** The power spectrum is then divided into $N$ partitions, where $N$ is determined using constraints around the error obtained in the previous step. Each partition represents a frequency interval in which the modeling error of Eq.(3) is located in between an empirical threshold and its multiples. Fig.(2), illustrates partitioning to different frequency ranges according to the modeling error rate.

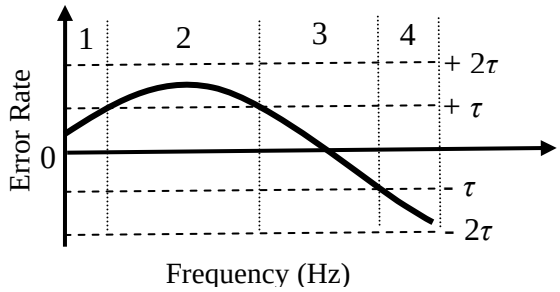


Figure 2: The modeling error is partitioned into 4 successive segments according to an empirical threshold $\tau$.

In Fig.(2), number of partitions is a function of the threshold $\tau$. This threshold represents the level of accuracy the algorithm intends to do partitioning. In other words, it is the maximum fluctuation allowed in the texture of each partition. In this step, we rewrite Eq.(3) in this form,

$$P_{pw}(f) = P_{E1}(f) + P_{E2}(f) + ... + P_{EN}(f) \quad (6)$$

in Eq.(6), each element on the right side is a single power law in form of Eq.(1), each of which has a characteristic frequency fixed at the partition's median frequency. This implies that the magnification in each frequency range is fixed so that the texture in local areas is represented uniformly with respect to the local energy distributions.

**Step 3:** In this step, logarithm of the error represented by the Eq.(4) is differentiated with respect to the parameters of each model. By considering the median frequency of each partition as the characteristic frequency for each model a standard least square is formed. Similar to the algorithm presented in [1], model parameters can be computed by solving a linear set of equations in this form,

$$\begin{bmatrix} a_{11} & a_{12} & a_{13} \\ a_{21} & a_{22} & a_{23} \\ a_{31} & a_{32} & a_{33} \end{bmatrix} \begin{bmatrix} G_i \\ Q_i \\ C_i \end{bmatrix} = \begin{bmatrix} b_1 \\ b_2 \\ b_3 \end{bmatrix} \quad (7)$$

in Eq.(7), $Q_i = q_i + g_i$, $G_i = g_i$, and $K_i = c_i f_{0i}^{2qi}$ represent extracted parameters for each partition, where the least square solution is minimized for the $i^{th}$ partition. The $a$ and $b$ terms are a function of characteristic frequency and partition frequency range [1]. The characteristic frequency is estimated and the frequency ranges are fixed when Eq.(7) is used. Again we note that having a fix characteristic frequency, related to the median frequency of each partition, implies same magnification into the textural information. The extracted parameters can be represented in this form.

$$\Theta = \begin{bmatrix} q_N & g_N & c_N & f_N \\ : & : & : & : \\ q_2 & g_2 & c_2 & f_2 \\ q_1 & g_1 & c_1 & f_1 \end{bmatrix} \quad (8)$$

The overall piecewise modeling error can be computed by adding up all the errors obtained in the previous step in this form,

$$E_T = \sum_{i=1}^{N} \sum_{j=1}^{M_i} e_{ij} \quad (9)$$

in Eq.(9), $N$ is the number of partitions and $M_i$ is the number of samples in the $i^{th}$ partition. As previously stated, this error rate is a measure of the fitting accuracy and also represents the degree of self-affinity.

## 3. METHODS AND MATERIALS

### 3.1 Simulations

MESs were simulated using a general purpose structural model-based simulator [6]. For this experiment, 4 sets of MESs were simulated, with each set consisting of 10 MESs, which are 3 s long. In first and second sets, MESs have a low CV (3 m/s) and normal CV (5.5 m/s), respectively. In third and fourth sets, MESs have deep active MUs (35 mm) and an average active depth (20 mm), respectively. The simulation parameters were used considering [4], summarized in Table I.

### 3.2 Processing

The amplitude of the MESs was normalized before power spectrum estimation. The power spectrum of the MES was estimated using Welch's method [7]. For averaging, a Hamming window with a temporal width of 256 samples was applied, with a 50% overlap between windows.

To determine an optimal threshold for the partitioning algorithm, different thresholds ranging between 0.001 to 1 % of the total power were applied. It was observed that the partitions have consistent boundaries approximately every 60 Hz. To unify the number of the partitions for all signals we also performed a uniform partitioning and divided the power spectrum to 5 partitions, each of which contains 20 % of the total power. This was done as an alternative to using a fixed threshold, where a different number of partitions might be obtained within a set of 10 MESs.

TABLE I: MYOELECTRIC SIGNAL SIMULATION PARAMETERS

| | |
|---|---|
| Source Duration | 3 msec |
| Conduction Velocity | 3 and 5.5 m/s |
| Num. of Fibers in MU | 40 |
| Innervation Zone to Electrode Distance | 35 mm |
| Length of Fiber | 210 mm |
| Termination Dispersion | 1 mm |
| Innervation Zone Dispersion | 1 mm |
| Depth of MU (deviation) | 25 or 35 mm ($\sigma$ = 2.5 mm) |
| Num. of MU | 50 |
| Firing Rate (deviation) | 20 Hz ($\sigma$ = 3 Hz) |
| Sampling Rate | 20 kHz |

## 4. RESULTS AND DISCUSSION

Fig.(1) shows the power spectrum and the obtained piecewise model by the new partitioning algorithm when CV = 3 m/s. Table II summarizes all the experimental results. Experimental results, particularly the modeling error, show a significant improvement when using the new algorithm. The new partitioning algorithm is also very flexible for using different frequency ranges.

Skewness or compression, results in a degraded self-affinity of the signal; therefore, estimated parameters using one single model becomes highly erroneous, residing at the higher edges of the error convex. In such cases, the parameters describe the dominant complexity, which is not accurately related to the texture of neither the compressed or regular regions. Restricting the adaptation to partitions, results in a better accuracy where single level dominant complexity indicators of the power law are insufficient for characterizing the whole power spectrum behavior (multi-complexity). This implies multi-fractal characteristics. In other words the whole power spectrum is representing more than one textural characteristic and different frequency ranges might possess specific coarseness qualities associated with them. This novel partition algorithm minimizes the limitations for expressing a power spectrum in form of mono-fractals by reducing the frequency range in which the power law must be valid. Local characteristics can now be represented with dominant complexity indicators with negligible error rates.

TABLE II: MODELING MEAN ERROR AND STANDARD DEVIATION

| | Piecewise Power Laws | Single Power Law |
|---|---|---|
| Low CV (3 m/s) | 0.6 % ($\sigma$ = 0.1 %) | 15 % ($\sigma$ = 5.0 %) |
| High depth (35 mm) | 0.7 % ($\sigma$ = 0.1 %) | 16 % ($\sigma$ = 5.3 %) |
| CV = 5.5 m/s and MU depth = 25 mm | 0.4 % ($\sigma$ = 0.1 %) | 9.1 % ($\sigma$ = 3.1 %) |

## 5. CONCLUSIONS AND FUTURE DIRECTIONS

A novel partitioning algorithm for piecewise modeling using general self–affine power laws has been introduced. We showed an application of this algorithm for MES and demonstrate the improved modeling accuracy for low CV and high depth of active MUs, which causes compression and/or skewness in the power spectrum curvature.

These results are promising a very solid ground for bio-fractal signal processing with their ability in accurately representing complicated power spectrums in form of statistical self-affinity. We are currently experimenting with this algorithm on speech and electroencephalography signals. As well, we are continuing our research on MESs, aimed for fatigue and joint angle studies.

## ACKNOWLEDGMENT

This work was supported by the Natural Sciences and Engineering Research Council (NSERC) of Canada.

## REFERENCES

[1] M.J. Turner, J.M. Blackledge and P.R. Andrews, *Fractal geometry in digital imaging.* Academic Press, London, UK, 1998.

[2] M. Talebinejad, A.D.C. Chan, A. Miri and R. Dansereau, "Fractal analysis of myoelectric signals: a novel power spectrum-based method," *accepted to J Electromyography Kinsiol,* Sept. 2007.

[3] M. Talebinejad, A.D.C. Chan, A. Miri and R. Dansereau, "Effects of force and joint angle on fractal parameters of the myoelectric signals," *Proc IEEE Intl Conf Eng Med Biol Soc*, pp. 3423-3426, 2006.

[4] R. Merletti and P.A. Parker, *Electromyography: Physiology, Engineering and Non-Invasive Applications.* Wiley-IEEE Press, New York, USA, 2004.

[5] M. Talebinejad, A.D.C. Chan, and A. Miri, "Effects of conduction velocity and spectral compression on fractal parameters of the myoelectric signals," *Proc Cdn Med Biol Eng Conf*, Toronto, CANADA, M0087, 2007.

[6] N. Jiang, "Modelling of motor unit innervation process correlation and motor unit common drive in human skeletal muscles," M.Sc.E. Thesis, University of New Brunswick, Fredericton, NB, CANADA, 2004.

[7] H. Monson, *Statistical digital signal processing and modeling*. Wiley Press, New York, USA, 1996.